PRAMANA — journal of physics

Vol. 85, No. 4
October 2015
pp. 605–616

Spectral intensity distribution of trapped fermions

SUDEEP KUMAR GHOSH
Centre for Condensed Matter Theory, Department of Physics, Indian Institute of Science, Bangalore 560 012, India
E-mail: sudeep@physics.iisc.ernet.in

MS received 18 May 2014; revised 2 August 2014; accepted 4 August 2014
DOI: 10.1007/s12043-014-0903-6; ***e*Publication:** 29 January 2015

Abstract. To calculate static response properties of a many-body system, local density approximation (LDA) can be safely applied. But, to obtain dynamical response functions, the applicability of LDA is limited bacause dynamics of the system needs to be considered as well. To examine this in the context of cold atoms, we consider a system of non-interacting spin-$\frac{1}{2}$ fermions confined by a harmonic trapping potential. We have calculated a very important response function, the spectral intensity distribution function (SIDF), both exactly and using LDA at zero temperature and compared with each other for different dimensions, trap frequencies and momenta. The behaviour of the SIDF at a particular momentum can be explained by noting the behaviour of the density of states (DoS) of the free system (without trap) in that particular dimension. The agreement between exact and LDA SIDFs becomes better with increase in dimensions and number of particles.

Keywords. Trapped fermions; local density approximation; spectral intensity distribution function.

PACS Nos 03.75.Ss; 32.30.Bv

1. Introduction

Since cold atomic systems provide clean artificial systems and have wide tunability of parameters, theoretical and experimental research on these systems have been very active in recent years. Overcoming some initial difficulties like entropy removal, creation of gauge fields etc., these systems have emerged as clean quantum emulators. The interaction between the particles can be tuned by changing the magnetic field across a Feshbach resonance. Due to this tunability of interactions, desired many-body quantum Hamiltonians can be simulated. Thus, cold atomic systems allow us to study interesting quantum many-body physics in a controlled environment when it is difficult to prepare natural systems with desired parameter regimes and enable us to create strongly correlated systems of interest in many areas like condensed matter physics, nuclear physics, high-energy physics, etc.

The temperature being very low, trapped cold atomic gases are in the quantum degeneracy regime. In this regime bosons condense to a Bose–Einstein condensate (BEC) [1]. By trapping the BEC in an optical potential and suppressing charge fluctuations by increasing the depth of the optical lattice, transition from a superfluid BEC to a Mott insulator had been realized [2]. Similarly, in degenerate Fermi gases, cross-over from a condensate of very weakly bound Cooper pairs in the Bardeen–Cooper–Schrieffer (BCS) state to a condensate of tightly bound Bosons in the BEC state, was obtained by tuning the interaction between the fermions across unitarity [3]. Interesting quantum many-body physics occurs in the presence of magnetic fields but because cold atoms are neutral, gauge fields are needed to be produced artificially [4–6]. In fermions, synthetic non-Abelian gauge fields have many interesting consequences like emergence of novel states [7], amplification of interaction etc. [8–10]. Experimentally, these synthetic non-Abelian gauge fields have been realized recently [11,12].

Another major achievement of the last decade is the development in the field of photoemission spectroscopy [13,14]. Photoemission spectroscopy enables one to probe the occupied single-particle states of a fermionic system. The usual photoemission spectroscopy was generalized to the case of cold atomic systems using radio frequency photoemission spectroscopy [15]. In Fermi gases this technique reveals interesting many-body effects like the pseudogap phenomenon [16–19].

The spectral function is a very important quantity for a many-body system because it reveals many important aspects like excitations of the system. In radio frequency photoemission spectroscopy, this quantity is routinely measured [17]. The static response properties of a many-body system are well captured within LDA because the dynamics of the system is not involved in this case. To account for the dynamics of the system in obtaining dynamical response functions, there are different versions of LDA like the time-dependent LDA (TDLDA). But their applicability depends on the adiabaticity of the dynamics of the system [20,21]. Let $\chi(\omega^+, \mathbf{q})$ be the response function of a many-body system, where $\mathbf{q}$ is the momentum and ω is the frequency. Then, to obtain the static response function $\lim_{\omega\to 0}\chi(\omega^+, \mathbf{q})$ or the average static response $\lim_{\omega\to 0}\lim_{\mathbf{q}\to 0}\chi(\omega^+, \mathbf{q})$, LDA can be applied. But, in obtaining the full dynamical response function $\chi(\omega^+, \mathbf{q})$, applicability of LDA is limited because of the reason described earlier.

Even a system of non-interacting fermions in the presence of trap has many interesting characteristics as the trapping potential explicitly breaks the spatial translational invariance [7,22–25]. The chemical potential and thermodynamic quantities such as specific heat show oscillation as a function of the number of particles due to the finite degeneracy of the energy eigenstates of the isotropic harmonic oscillator [26–28]. So, we take the viewpoint that this ideal Fermi system, in the presence of an isotropic harmonic trapping potential, is very interesting and we consider spin-$\frac{1}{2}$ version at zero temperature. We investigate the performance of LDA with respect to the exact case by calculating a dynamical response function of the system as an example. The dynamical response function, is the spectral intensity distribution function (SIDF). This SIDF is calculated exactly using LDA in any dimension for various parameter regimes. The results obtained using the two techniques are compared for different momenta, different trap frequencies and different number of particles in 1, 2 and 3 dimensions. We have found that as the dimension increases the agreement between the exact and LDA SIDFs gets better. Moreover, increase in the

number of particles makes LDA better in higher dimensions. In the following section, we describe the system under consideration and formulate the problem.

2. Description of the system

We consider a system of non-interacting spin-$\frac{1}{2}$ fermions trapped in a harmonic potential of frequency ω_0. The Hamiltonian of the system is

$$\hat{\mathcal{H}} = \frac{\hat{\mathbf{p}}^2}{2m} + \frac{1}{2}m{\omega_0}^2\hat{\mathbf{r}}^2 \ , \tag{1}$$

where m is the mass of fermions. Taking m and the Planck's constant ($\hbar$) to be unity, the Hamiltonian operator in momentum space can be written as

$$\hat{\mathcal{H}} = -\frac{1}{2}{\omega_0}^2\frac{\partial^2}{\partial\hat{\mathbf{p}}^2} + \frac{1}{2}\hat{\mathbf{p}}^2 \ . \tag{2}$$

The one-dimensional harmonic oscillator eigenstates in momentum space can be labelled by a quantum number n (n is an integer). They are

$$\phi(n,k) = \frac{1}{\sqrt{2^n n!}}\left(\frac{1}{\pi\omega_0}\right)^{1/4}\exp\left(-\frac{k^2}{2\omega_0}\right)H_n\left(\frac{k}{\sqrt{\omega_0}}\right) \tag{3}$$

with energy $\varepsilon_n = (n+\frac{1}{2})\omega_0$. The eigenstates of the harmonic oscillator in d-dimension are products of d one-dimensional harmonic oscillator eigenfunctions and are labelled by a set of d integers $\{\mathbf{n}\}$. In momentum space representation they are given by

$$\langle\mathbf{k}|\mathbf{n}\rangle = \psi(\mathbf{n},\mathbf{k}) = \prod_{i=1}^{d}\phi(n_i,k_i) \tag{4}$$

with energies $\varepsilon(\mathbf{n}) = \sum_{i=1}^{d}(n_i+\frac{1}{2})\omega_0$. In calculating the SIDF exactly these eigenfunctions are used while in LDA the harmonic potentials are used to obtain approximate local quantities.

3. Calculation of SIDF

The SIDF is an important response function because it contains information about many-body effects in the system. At zero temperature, the SIDF is calculated using two techniques: (1) LDA and (2) exact method. Complete analytical expressions for SIDF is obtained using LDA in any dimension and exact SIDF is obtained numerically. We note that there are two important energy scales in the problem: trap centre chemical potential (μ_0) and the frequency of the harmonic potential (ω_0).

3.1 *Calculation using LDA*

Within LDA, we take into account the effect of trap potential by making the chemical potential μ of the system a 'local variable' [26]. This local chemical potential $\mu(\mathbf{r})$

determines the density of particles $\rho(\mathbf{r})$ at a point in space $\mathbf{r}$ and they are related by the equation of state. As a function of μ_0, $\mu(\mathbf{r})$ is given by

$$\mu(\mathbf{r}) + \frac{1}{2}\omega_0^2 r^2 = \mu_0. \tag{5}$$

The SIDF calculation within LDA is, therefore, two-fold: first obtain μ_0 as a function of ω_0 and number of particles (N) and then calculate $\mu(\mathbf{r})$ to obtain SIDF.

3.1.1 *Calculation of the trap centre chemical potential*: Let there be N particles in the trap which form a cloud of radius R_0. Then in d-dimensions ($d \geq 2$) we have

$$\int_0^{R_0} \mathrm{d}\mathbf{r}\ \rho(\mathbf{r}) = N, \tag{6}$$

where $\rho(\mathbf{r})$ is the density of particles at position $\mathbf{r}$. Considering spherical symmetry in the problem we note that $\rho(\mathbf{r})$ depends only on r, which leads to

$$C(d) \int_0^{R_0} \mathrm{d}r\ r^{d-1}\rho(r) = N \tag{7}$$

with $C(d) = 2\pi^{d/2}/\Gamma(d/2)$. The trap centre chemical potential μ_0 and the radius of the cloud R_0 is related as

$$\mu_0 = \frac{1}{2}\omega_0^2 R_0^2. \tag{8}$$

If $g(\mathbf{k})$ is the density of state (DoS) of non-interacting free spin-$\frac{1}{2}$ particles in $\mathbf{k}$-space then $g(\mathbf{k}) = 2(V/(2\pi)^d)$ (the factor 2 comes from spin degeneracy and V is the volume of the d spatial dimension) in d dimensions. So, for $d \geq 2$

$$\int_0^{k_\mathrm{F}} \mathrm{d}\mathbf{k}\ g(\mathbf{k}) = N, \tag{9}$$

where k_F is the Fermi momentum of the system. The density of particles ρ is therefore

$$\rho = \frac{2C(d)}{d(2\pi)^d}(2\mu)^{d/2}, \tag{10}$$

where μ is the chemical potential of the free Fermi gas. This is the equation of state of the free Fermi gas in $d(\geq 2)$ dimensions. Plugging eq. (5) in eq. (10), the spatial density of the system within LDA can be written as

$$\rho(\mathbf{r}) = \frac{2C(d)}{d(2\pi)^d}(2\mu_0 - \omega_0^2 r^2)^{d/2}. \tag{11}$$

Substituting eq. (11) in eq. (7) and then using eq. (8), we obtain a relation among the variables μ_0, ω_0 and N in d dimensions ($d \geq 2$)

$$\left(\frac{2\mu_0}{\omega_0}\right)^d = \frac{N}{X(d)}, \tag{12}$$

where

$$X(d) = \frac{\sqrt{\pi}}{d(2^{2d-2})\Gamma(\frac{d}{2})\Gamma(\frac{d+1}{2})}.$$

Similarly, for a system of N particles in one dimension

$$\int_{-k_F}^{k_F} \mathrm{d}\mathbf{k}\; g(\mathbf{k}) = N \Rightarrow \sqrt{2\mu} = \frac{\pi\rho}{2}. \tag{13}$$

The spatial density of the trapped particles $\rho(r)$ obtained in the same way is

$$\rho(r) = \frac{2\omega_0}{\pi}\sqrt{R_0^2 - r^2}, \tag{14}$$

and we have

$$\int_{-R_0}^{R_0} \mathrm{d}r\; \rho(r) = N. \tag{15}$$

The above equation then leads to 1d version of eq. (12) as

$$\frac{2\mu_0}{\omega_0} = N. \tag{16}$$

Combining eqs (12) and (16), the trap centre chemical potential μ_0, the trap frequency ω_0 and the number of particles N in any dimension d are related as

$$X(d)(\omega_0 R_0^2)^d = N. \tag{17}$$

This relation is used to calculate the local chemical potential.

3.1.2 *Obtaining the SIDF within LDA*: The single-particle spectral function of a system with dispersion relation $\epsilon(\mathbf{k})$ is

$$A(\mathbf{k}, \omega) = \delta(\omega - \epsilon(\mathbf{k})). \tag{18}$$

In LDA, the SIDF is obtained by adding local single-particle spectral functions with suitable spectral weights. We approximate the free particle dispersion $\epsilon(\mathbf{k})$ to a local dispersion $\epsilon(\mathbf{r}, \mathbf{k})$ at every position $\mathbf{r}$ in space as

$$\epsilon(\mathbf{r}, \mathbf{k}) = \frac{k^2}{2} + \frac{1}{2}\omega_0^2 r^2, \tag{19}$$

for the trapped system. The LDA form of the local single-particle spectral function $A(\mathbf{r}, \mathbf{k}, \omega)$ is then

$$A(\mathbf{r}, \mathbf{k}, \omega) = \delta(\omega - \epsilon(\mathbf{r}, \mathbf{k})). \tag{20}$$

So, the total SIDF $I(\mathbf{k}, \omega)$ is obtained as

$$I(\mathbf{k}, \omega) = \int \mathrm{d}\mathbf{r}\; W(\mathbf{r}, \mathbf{k}) A(\mathbf{r}, \mathbf{k}, \omega), \tag{21}$$

where $W(\mathbf{r}, \mathbf{k})$ is the spectral weight of the local single-particle spectral function at position $\mathbf{r}$. In d dimensions it is given by

$$W(\mathbf{r}, \mathbf{k}) = \frac{1}{(2\pi)^d}\Theta(\mu_0 - \epsilon(\mathbf{r}, \mathbf{k})).$$

In one dimension, we use the relation between the trap centre chemical potential μ_0 and the number of particles N from eq. (16) in eq. (21) to obtain

$$I(k,\omega) = \frac{1}{2\pi}\int_{-r_k}^{r_k} \mathrm{d}r\ \delta\left(\omega - \frac{k^2}{2} - \frac{1}{2}\omega_0^2 r^2\right)\Theta(\mu_0 - \omega), \tag{22}$$

where

$$r_k = \frac{\sqrt{2\mu_0 - k^2}}{\omega_0}.$$

This equation gives in one dimension the LDA form of the SIDF

$$I(k,\omega) = \frac{\Theta(\mu_0 - \omega)\Theta(\omega - \frac{k^2}{2})}{\pi\omega_0\sqrt{2\omega - k^2}}\ . \tag{23}$$

In the same way as above in d-dimensions ($d \geq 2$) using eq. (12) in eq. (21) we get

$$I(\mathbf{k},\omega) = \frac{C(d)}{(2\pi)^d}\int_0^{r_k} \mathrm{d}r\ r^{d-1}\delta\left(\omega - \frac{k^2}{2} - \frac{1}{2}\omega_0^2 r^2\right)\Theta(\mu_0 - \omega), \tag{24}$$

which then gives the SIDF for spin-$\frac{1}{2}$ particles in d-dimensions ($d \geq 2$) as

$$I(\mathbf{k},\omega) = \frac{C(d)}{(2\pi)^d}\left(\frac{R_m^{d-2}}{\omega_0^2}\right)\Theta(\mu_0 - \omega)\Theta\left(\omega - \frac{k^2}{2}\right), \tag{25}$$

where

$$R_m = \sqrt{\frac{2\omega - k^2}{\omega_0^2}}.$$

The form of the SIDF $I(\mathbf{k},\omega)$ in any dimension d from eqs (23) and (25) can therefore be written as

$$I(\mathbf{k},\omega) = \frac{C(d)}{(2\pi)^d}\left(\frac{R_m^{d-2}}{\omega_0^2}\right)\Theta(\mu_0 - \omega)\Theta\left(\omega - \frac{k^2}{2}\right), \tag{26}$$

where

$$R_m = \sqrt{\frac{2\omega - k^2}{\omega_0^2}} \quad \text{and} \quad C(d) = \frac{2\pi^{d/2}}{\Gamma(d/2)}.$$

Due to the conservation of number of particles N, the SIDF obeys the following sum rule:

$$\int \mathrm{d}\mathbf{k}\ \mathrm{d}\omega\ I(\mathbf{k},\omega) = N. \tag{27}$$

By using the expression of $I(\mathbf{k},\omega)$ from eq. (26) and carrying out integration over momentum and energy we see that the SIDFs obtained using LDA indeed obey the sum rule given by eq. (27).

3.2 *Exact calculation*

To calculate the SIDF exactly we use the harmonic oscillator basis set given by eq. (4). In terms of the eigenstates labelled by a set of quantum numbers $\{\mathbf{n}\}$ with energies $\varepsilon(\mathbf{n})$, the SIDF is

$$I(\mathbf{k}, \omega) = \sum_{\{\mathbf{n}\}} |\langle \mathbf{n}|\mathbf{k}\rangle|^2 \delta(\omega - \varepsilon(\mathbf{n})), \tag{28}$$

where the sum is over all the occupied states. The SIDF thus obtained is spherically symmetric. Orthonormality of the eigenfunctions of the harmonic oscillator can be used to show that the sum rule given by eq. (27) is satisfied. By using these eigenfunctions and carrying out the summation over all the occupied states for a fixed number of particles N, we obtain the SIDF in any dimension. The summation is performed numerically by broadening the delta function as a Lorentzian of 'suitable width'. As an approximation to the delta function $\delta(x)$, we use the Cauchy–Lorentz probability density function

$$\mathcal{L}(x, \eta) = \frac{1}{\pi} \frac{\eta}{x^2 + \eta^2}, \tag{29}$$

where η is the half-width at half-maximum (HWHM) of $\mathcal{L}(x, \eta)$. As $\eta \to 0$, the Lorentzian distribution $\mathcal{L}(x, \eta)$ approaches the delta function distribution $\delta(x)$, where η is a phenomenological parameter which needs to be chosen properly. As the energy levels of an isotropic harmonic oscillator are degenerate, we account for suitable degeneracies of these levels and choose the number of particles such that the highest occupied harmonic oscillator level is completely filled. The degeneracy g_d^n of the nth energy eigenstate of a d-dimensional isotropic harmonic oscillator can be calculated from the following recursion relation:

$$g_d^n = \sum_{n_1=0}^{n} g_{d-1}^{n-n_1} \quad \text{with} \quad g_1^n = 1. \tag{30}$$

Using this relation, the expression for the degeneracy is obtained to be

$$g_d^n = \frac{\Gamma(n + d)}{\Gamma(d)\Gamma(n + 1)}\ , \tag{31}$$

and if the highest occupied energy level $n = \nu_{\max}$, the total number of particles in the system (including spin degeneracy) is

$$N_d^{\nu_{\max}} = 2 \sum_{n=0}^{\nu_{\max}} g_d^n = \frac{2\,\Gamma(\nu_{\max} + d + 1)}{\Gamma(d + 1)\Gamma(\nu_{\max} + 1)}\ . \tag{32}$$

The following section contains discussions of our results.

4. Results and discussion

It is noted from eq. (26) that the behaviour of the SIDF at a particular momentum is similar to the DoS of the system as a function of energy without the trapping potential at that particular dimension. So, we expect the behaviour of SIDF of the trapped spin-$\frac{1}{2}$ fermionic system to be similar to the corresponding DoS of the free spin-$\frac{1}{2}$ fermionic

system. The DoS, $g(\omega)$, as a function of ω of a free spin-$\frac{1}{2}$ fermionic system in 1, 2 and 3 dimensions, is proportional to $1/\sqrt{\omega}$, constant and is proportional to $\sqrt{\omega}$, respectively. Thus $I(\mathbf{k}, \omega)$ of the trapped system at a particular momentum is expected to have similar behaviour in the corresponding dimensions. The dynamical response function $I(\mathbf{k}, \omega)$ encodes the dynamics of the system and have information about the excitations of the system. To capture the dynamical nature within LDA, there are different forms of LDA such as the TDLDA but their domain of applicability is limited by the slowness of dynamics of the system [20,21]. The simplest version of LDA (i.e., the time-independent LDA) was used here to calculate the dynamical response function $I(\mathbf{k}, \omega)$ and its behaviour was studied in different parameter regimes within this approximation. The SIDF obtained using LDA was compared with the corresponding exact numerical results for different values of $k = |\boldsymbol{k}|$ due to the spherical symmetry. We discuss their behaviours only for the physical dimensions 1, 2 and 3 although in principle the SIDFs can be calculated using these two methods in any dimension.

Owing to the limitation set by the trap centre chemical potential and the conservation of energy, energy range of the LDA SIDF is limited to a certain window and it is non-zero only within this energy window. Although exact SIDF is large in this window, it has small spectral weight outside as well. Because of the energy time uncertainty principle, in a physical context with interaction, if the excitations of the system have finite lifetime, then this leads to spectral broadening. The phenomenological broadening parameter can, therefore, be related to the finite lifetime of the quasiparticle excitations of the system. The minimum energy difference between the harmonic oscillator energy levels is ω_0 and for comparing with the LDA SIDF, we have chosen the value of η to be $\eta/\omega_0 = 1/2$ in exact calculation.

The comparison between the SIDFs in one dimension is shown in figure 1 at $k = 0$ (figure 1a) and $k = (k_{\mathrm{F}}^0/2)$ (figure 1b) for $N = 100$, 250 and 500 which correspond to highest occupied energy level $\nu_{\max} = 49$, 124 and 249, respectively. Here, k_{F}^0 is the Fermi wave vector set by the trap centre chemical potential $\mu_0 = ((k_{\mathrm{F}}^0)^2/2)$. As N is increased, the oscillations in the exact SIDF increases. With the change in momentum, the threshold

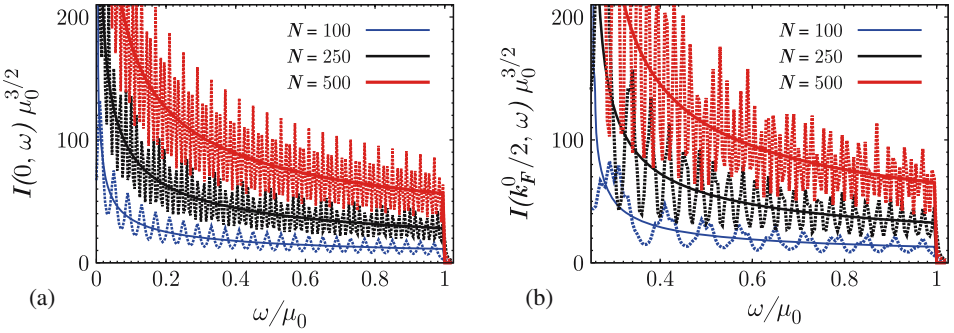

Figure 1. The SIDF as a function of energy for a system of spin-$\frac{1}{2}$ particles in one dimension with the broadening of the Lorentzian distribution $(\eta/\omega_0) = 0.5$ used in the exact calculation. The dotted curves denote exact results and the solid curves denote LDA results. (**a**) Shows the SIDF at zero momentum and (**b**) shows the SIDF at a different value of momentum $k = k_{\mathrm{F}}^0/2$. The exact SIDF has spectral weights outside the LDA window and they have $1/\sqrt{\omega}$ like dependence.

for the SIDF in LDA result is expected to change because the free-particle contribution to energy is changed but there is also a high frequency cut-off in the LDA spectrum due to the trap centre chemical potential. The exact SIDF has large weight within the LDA window and relatively small weight outside it; also at momentum $k = k_F^0/2$ but with suppressed fluctuations. It is seen from this figure that within the corresponding window of energy, the behaviours of the SIDFs for zero and finite momentum are similar.

The expected constant behaviour of the SIDF in two dimensions is clearly seen from figure 2. At zero and finite momenta the comparisons of exact and LDA SIDFs are shown in figures 2a and 2b, respectively for $N = 110$, 506 and 1056 which correspond to $\nu_{\max} = 9$, 21 and 31, respectively. It is noted that at half of the Fermi momentum, LDA gives a better description than that at the zero momentum. As expected, the LDA window becomes smaller due to the increase in the free-particle energy for the finite momentum case and the comparison with the exact results becomes better for larger number of particles.

In three dimensions, $I(\mathbf{k}, \omega)$ at a particular momentum k as a function of ω, has an overall $\sqrt{\omega}$ dependence which is as expected. This is seen from figure 3 with $N = 112$, 572 and 1120 which correspond to $\nu_{\max} = 5$, 10 and 13, respectively at $k = 0$ (figure 3a) and $k = (k_F^0/2)$ (figure 3b). LDA SIDFs are in a particular window whereas exact spectra have some small spectral weights outside as well. The finite-momentum SIDFs are similar to that of the zero-momentum results although for finite momentum the oscillations get suppressed in the exact SIDF. In this dimension, as N increases, LDA becomes better than that for 1D and 2D cases.

The oscillations seen in the exact SIDFs for a fixed number of particles can be attributed to the discrete nature of the harmonic oscillator spectrum. The periods of these oscillations vary with changing N due to the change in the trap centre chemical potential. Although, for comparison we have chosen a particular value of $\eta = \omega_0/2$, with smaller values of η the oscillations in the exact SIDFs increase and for very small values of η, the disagreement between the exact and LDA SIDFs increases and exact SIDFs become vanishingly small. We also see step-like behaviour when we calculate the exact SIDF as a function of N at fixed ω and $|\mathbf{k}|$, due to the finite degeneracy of the harmonic oscillator levels. Similar behaviours were also seen earlier in [27,28] for this system in its

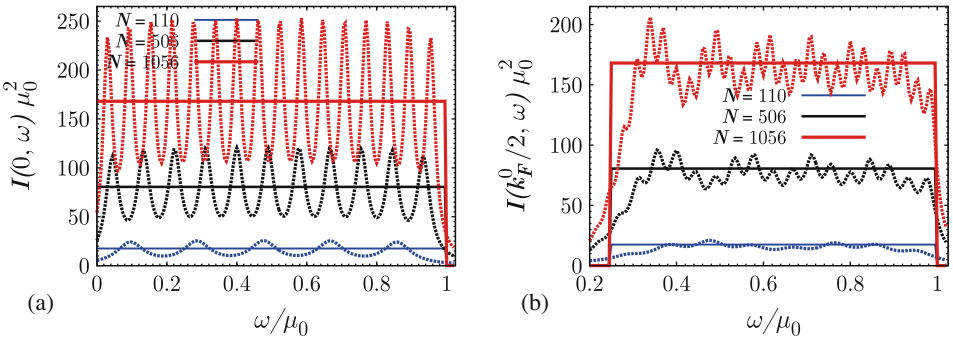

Figure 2. Comparison of exact (dotted) and LDA (solid) SIDFs in 2d. SIDFs for $k = 0$ and $k = k_F^0/2$ are shown in (**a**) and (**b**) respectively. Here, $(\eta/\omega_0) = 0.5$. It is seen that the LDA SIDF is constant within a window but exact SIDF has weight outside the window as well. Smaller fluctuation in the exact SIDF is seen in finite momentum case.

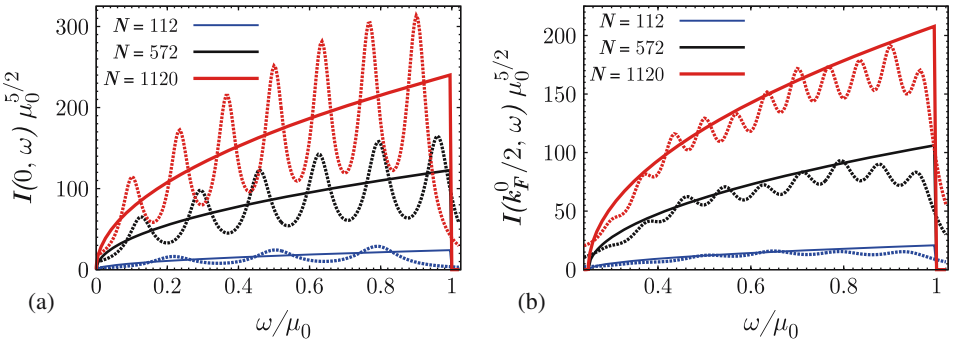

Figure 3. The three-dimensional SIDF as a function of energy at fixed momentum is shown. The value of the phenomenological parameter used in the exact calculation is $(\eta/\omega_0) = 0.5$ with exact and LDA results denoted by dotted and solid curves, respectively. (**a**) Shows the SIDF at zero momentum and (**b**) shows the SIDF at momentum $k = k_F^0/2$. It is seen that the SIDF has an overall $\sqrt{\omega}$ dependence and the exact spectra have weights outside the LDA window. The fluctuations in the exact SIDF are smaller for the case of finite momentum.

thermodynamic quantities. From [27,28], it is seen that thermodynamic quantities of this system oscillates as a function of N and continuum approximation or LDA gives better results at higher temperatures. But for very small temperatures, the disagreement with the continuum approximation increases and the exact results become vanishingly small. So, the temperature plays a similar role as the broadening parameter η.

Figure 4 shows the full SIDF spectrum calculated using LDA in 1, 2 and 3 dimensions (in the contour plots figures 4a, 4b and 4c, respectively) as functions of both energy and momentum. The full spectrum has the same overall features as the fixed momentum case but now the behaviours at all momenta are seen. The two-dimensional spectrum clearly shows a contour separating the zero and non-zero regions. The nature spectra corresponding to one and three dimensions are opposite to each other as is expected, i.e., the 1D spectrum has small spectral weights at small momenta and high energy whereas the 3D spectrum has large spectral weights in this regime.

By radio frequency photoemission spectroscopy technique, the spectral density function of a many-body Fermi system is routinely measured [17]. Using spin-polarized Fermi gas to load the atoms to a single hyperfine state, a non-interacting Fermi system can be created [29]. For RF measurements done in this kind of system of ultradilute almost ideal Fermi gas, the SIDF of the system will have signatures as described earlier in the section. Hence, we see that although the exact dynamical response function $I(\mathbf{k}, \omega)$ has many interesting features, LDA captures essentially most of them quite accurately. We believe that our results will be useful to experimentalists and motivate further theoretical work.

5. Summary and outlook

In this paper, we have investigated how good is LDA in comparison to exact case in determining the dynamical response functions of an ultracold many-body Fermi system.

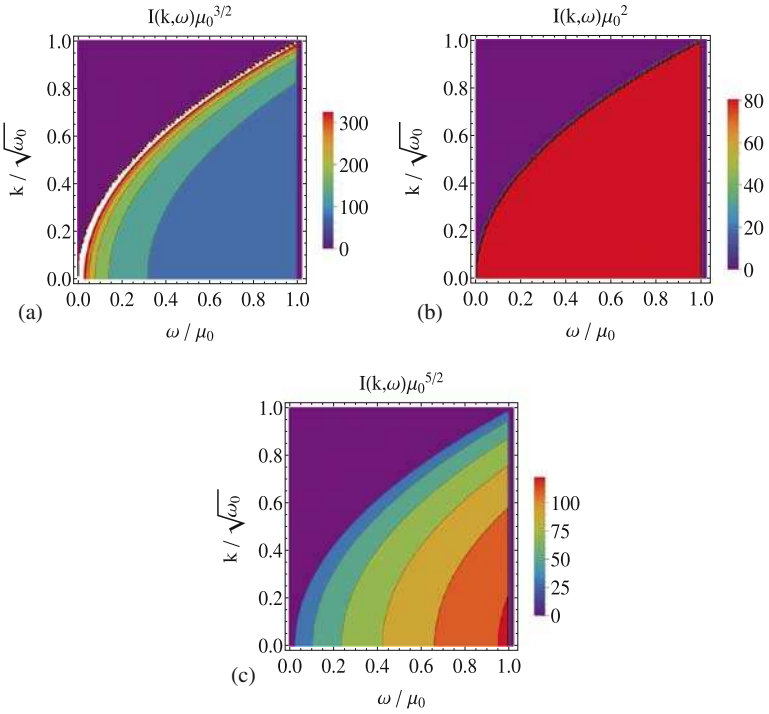

Figure 4. Contour plots of the full SIDF spectrum as functions of both momentum and energy calculated using LDA are shown. (**a**), (**b**) and (**c**) show the spectra for 1, 2 and 3 dimensions for $N = 500$, 506 and 572, respectively. The SIDF corresponding to two dimensions clearly shows that it is non-zero below a certain energy contour and is zero above it. The one-dimensional SIDF for small momentum and large energies has smaller values but the three-dimensional SIDF shows opposite behaviour.

We have considered a system of ultracold dilute non-interacting spin-$\frac{1}{2}$ Fermi gas in a harmonic trap at zero temperature. Identifying important scales in the problem, we have calculated one of the most important response functions, the SIDF of the system, exactly and using the simplest version of LDA (although there are other versions of LDA which have their own domain of applicability) in any dimension. The SIDFs at a particular momentum behave as the DoS of the system without trap in the corresponding dimension. We have shown that as the dimension increases the performance of LDA gets better and increase in number of particles makes LDA better in higher dimensions. Also, the intensity distribution function within LDA is non-zero only inside a certain range of energy window fixed by momentum and the trap centre chemical potential, but the exact spectra always have some small weight outside this window. We have shown the full dynamical SIDF as a function of both energy and momentum calculated using LDA and the expected behaviour is seen. We have described the experimental significance and importance of this paper. A novel future direction of this work will be to include repulsive interaction between the trapped spin-$\frac{1}{2}$ fermions and study the behaviour of the emerging Fermi liquid and its excitations in the presence of synthetic non-Abelian gauge fields.

Acknowledgements

The author acknowledges Vijay B Shenoy for extensive discussions. The financial support from CSIR, India through SRF grants is thankfully acknowledged.

References

[1] E A Cornell and C E Wieman, *Rev. Mod. Phys.* **74**, 875 (2002)
[2] M Greiner, O Mandel, T Esslinger, T W Hansch and I Bloch, *Nature* **415**, 39 (2002)
[3] C A Regal and D S Jin, *Adv. Atom. Mol. Opt. Phys.* **54**, 1 (2006)
[4] Y-J Lin, R L Compton, K J Garcia, J V Porto and I B Spielman, *Nature* **462**, 628 (2009)
[5] Y-J Lin, R L Compton, A R Perry, W D Phillips, J V Porto and I B Spielman, *Phys. Rev. Lett.* **102**, 130401 (2009)
[6] J Dalibard, F Gerbier, G Juzeliünas and P Öhberg, *Rev. Mod. Phys.* **83**, 1523 (2011)
[7] S K Ghosh, J P Vyasanakere and V B Shenoy, *Phys. Rev. A* **84**, 053629 (2011)
[8] J P Vyasanakere and V B Shenoy, *Phys. Rev. B* **83**, 094515 (2011)
[9] H Hu, L Jiang, X-J Liu and H Pu, *Phys. Rev. Lett.* **107**, 195304 (2011)
[10] J P Vyasanakere, S Zhang and V B Shenoy, *Phys. Rev. B* **84**, 014512 (2011)
[11] P Wang, Z-Q Yu, Z Fu, J Miao, L Huang, S Chai, H Zhai and J Zhang, *Phys. Rev. Lett.* **109**, 095301 (2012)
[12] L W Cheuk, A T Sommer, Z Hadzibabic, T Yefsah, W S Bakr and M W Zwierlein, *Phys. Rev. Lett.* **109**, 095302 (2012)
[13] R Comin and A Damascelli, arXiv preprint arXiv:1303.1438
[14] A Damascelli, Z Hussain and Z-X Shen, *Rev. Mod. Phys.* **75**, 473 (2003)
[15] T L Dao, A Georges, J Dalibard, C Salomon and I Carusotto, *Phys. Rev. Lett.* **98**, 240402 (2007)
[16] J T Stewart, J P Gaebler and D S Jin, *Nature* **454**, 744 (2008)
[17] J P Gaebler, J T Stewart, T E Drake, D S Jin, A Perali, P Pieri and G C Strinati, *Nature Phys.* **6**, 569 (2010)
[18] B Fröhlich, M Feld, E Vogt, M Koschorreck, W Zwerger and M Köhl, *Phys. Rev. Lett.* **106**, 105301 (2011)
[19] V Pietilä, *Phys. Rev. A* **86**, 023608 (2012)
[20] E K U Gross and W Kohn, *Phys. Rev. Lett.* **55**, 2850 (1985)
[21] K Yabana and G F Bertsch, *Int. J. Quant. Chem.* **75**, 55 (1999)
[22] L Pezzè, L Pitaevskii, A Smerzi, S Stringari, G Modugno, E de Mirandes, F Ferlaino, H Ott, G Roati and M Inguscio, *Phys. Rev. Lett.* **93**, 120401 (2004)
[23] E J Mueller, *Phys. Rev. Lett.* **93**, 190404 (2004)
[24] F Gleisberg, W Wonneberger, U Schlöder and C Zimmermann, *Phys. Rev. A* **62**, 063602 (2000)
[25] P Vignolo, A Minguzzi and M P Tosi, *Phys. Rev. Lett.* **85**, 2850 (2000)
[26] D A Butts and D S Rokhsar, *Phys. Rev. A* **55**, 4346 (1997)
[27] D J Toms, *Ann. Phys.* **320**, 487 (2005)
[28] J Schneider and H Wallis, *Phys. Rev. A* **57**, 1253 (1998)
[29] T Loftus, C A Regal, C Ticknor, J L Bohn and D S Jin, *Phys. Rev. Lett.* **88**, 173201 (2002)